Automated interpretation of top and base salt using deep convolutional networks

Oddgeir Gramstad and Michael Nickel, Schlumberger Stavanger Research*

Summary

We present a new automated workflow based on machine learning that can significantly reduce the amount of manual interpretation of top and base salt boundaries. Manual interpretation of salt boundaries on large seismic surveys with complex salt geometry is a time-consuming task. The interpreters manually pick a large number of surface control points line-by-line through the seismic volume. In this new method, we will replace the manual surface control picking with automation by using a machine learning approach. In the first part of the workflow we use a convolutional neural network that is designed to detect the top-of-salt boundary. Subsequently, a second convolutional network is then designed to detect the base of salt boundary. In both cases, the training data are picked as 2D subsections together with the corresponding manual interpretations in a specific seismic survey. The two trained networks are then evaluated both on the seismic data used in the training and on seismic data not used in the training. In both cases, we produce a top- and base-salt interpretation that coincides with the major parts of the manual interpretations. This new automated workflow has the potential to reduce the interpretation turnaround time of both top and base of salt.

Introduction

Salt body interpretation is a challenging task that significantly contributes to the critical path of a seismic processing project. A large number of surface control points is necessary to obtain a robust and detailed salt boundary interpretation, especially at the flanks and the base where the geometry is complex and the seismic signal quality is strongly varying. The surface control points are commonly picked manually by the interpreters by scanning through the seismic volume line-by-line (with a chosen offset) in inline and crossline directions. To obtain continuous 2D interpretations, the manual picking effort is typically supported by a 2D tracking algorithm that uses the picked surface control points as surface seed points. The last part of the workflow is to generate complete 3D interpretations by interpolating between the interpreted 2D lines. A proper salt interpretation used to segment the seismic velocity model is crucial to obtaining a good-quality image of the subsalt regions improving the identification and characterization of subsalt targets.

One way of further automating the above workflow for extracting explicit surfaces representing salt body boundaries was presented by Gramstad et al. (2017) and Haukaas et al. (2017). The first part of that workflow is an automated detection of surface control points along the top and base of the salt using a method that is inspired by search algorithms applied in identifying DNA sequences in biology. Subsequently, a surface extraction algorithm based on quality metrics is applied to laterally extend and connect the control points, resulting in signal-consistent surfaces with subsample precision. The second part of the workflow is an attribute-guided interpolation method used to guide the interpolation in zones where the seismic response is poor.

Here, we increase the degree of automation by further improving the workflow devised by Gramstad et al. (2017). We substitute the DNA-inspired approach for control point extraction along top and base salt by a supervised machine-learning approach based on deep learning of convolutional neural networks. This work is an extension of Gramstad et al. (2018). We also adapt the surface extraction algorithm to extract continuous top and base surfaces in 3D from the salt boundary interpretations produced by the convolutional neural networks. Waldeland et al. (2017) solved a segmentation problem by extracting the salt body as a 3D volume. We still focus on extracting (possibly multiple) top and base salt horizons to be able to deliver results that fit with the established overall workflow. Seismic imaging of salt bodies and their surroundings is an iterative process starting with a migration of the prestack seismic data using a velocity model flooded with sediment velocities only. This seismic data is called a sediment flood volume and the top of salt surface is interpreted on this volume. Having identified the top salt boundary, the velocity beneath it is changed to a salt velocity and a next migration is performed. Imaging the salt flanks and the salt base are improved in this step and the seismic volume is referred to as a salt flood volume. At this stage, the base salt boundary can be interpreted and migration proceeds to further improve the seismic image below the salt body. The method has been tested on real data from the Gulf of Mexico.

Supervised learning of convolutional neural networks

Convolutional neural networks have recently regained high popularity after their superior performance was demonstrated in several pattern recognition challenges. Applications range from object recognition in image scenes, segmentation of medical images, speech recognition and language understanding.

The main reasons for this success can be ascribed to increased compute capacity realized by the spread of powerful GPUs that allowed us to implement and train ever-more complex network architectures. In parallel,

10.1190/segam2018-2996306.1

significant advances were made in data science, making it feasible to robustly train the increasing number of network parameters. Given the success of this technology in other application domains one may project corresponding gains when applied to seismic interpretation tasks.

A convolution neural network is composed of several layers (N=10, 100, even 1000s) where each layer typically has the following basic building blocks: the input image is convolved with a number of filters (M) and, thus, enhances certain desired features in the input image. Contrarily to the widespread use of seismic attributes, the filters in a convolutional network are typically not pre-set but developed through training. The output of the convolutional filters is summed for each pixel location of the input image and then fed through a nonlinearity where now a rectified linear unit (ReLu) having a response

$$\text{ReLu:} \quad y = \begin{cases} x & x \geq 0 \\ 0 & x < 0 \end{cases}$$

is the most popular choice. The convolutional + ReLu layer may be followed by another or several such constructions or one may choose to subsample the obtained feature image by what is called a pooling operation. Stacking these basic layers renders a typical network architecture. The last layer(s) may be made by a fully connected layer where the whole feature image is multiplied with a filter matrix of equal size. Typically, this output is finally routed through a sigmoid function in case of a single class output or a softmax activation function in case of a multiclass output. Thus, maps having a value range [0,1] are obtained, indicating the probability of a pixel of the input image belonging to a specific class. The optimal network parameters are found by minimizing a cost function where the cross entropy between network output and the given labels i.e. its desired output is a popular choice. Once the network parameters are obtained the network can be very efficiently applied on other data sets with similar characteristics. Figure 1 shows the different building blocks used in a convolutional neural network (CNN).

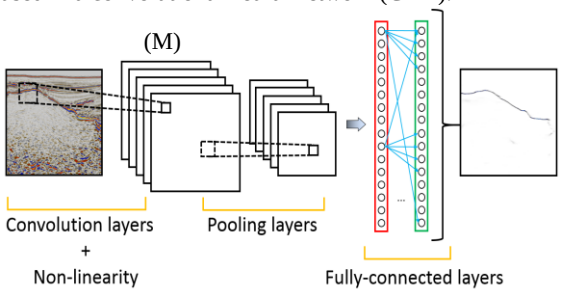

Figure 1: A convolutional neural network typically consists of a sequence of the following four main building blocks: convolutional layers, non-linearity layers, pooling layers and fully connected layers.

Training of a CNN for top salt interpretation

Projecting the success that CNNs show when applied in the analysis of, e.g., medical or real-world scene images, it should be possible to adapt this technology to detect the top of a salt body based on seismic input data. We test two different scenarios for top-of-salt detection. First, the CNN is trained based on a manually/semi-automatically picked top salt surface where 15% of the data are used in the training to determine the parameters of the CNN. The trained CNN is used to predict the top salt horizon on the entire survey.

The second scenario investigates whether the trained CNN is general enough to predict the top salt horizon of a nearby seismic survey that is not used in training the CNN.
Having available both a large sediment flood seismic volume and the corresponding top salt horizon generated through manual interpretation, a set of 2D crosslines evenly distributed over the survey are extracted to make up the training data. Each crossline is further subdivided into images of 128 by 128 pixels to serve as input to the network training (Figure 2). The output has the same format as the input where the pixels intersected by the top salt horizon are labelled '1' and the rest as '0' corresponding to the background class.

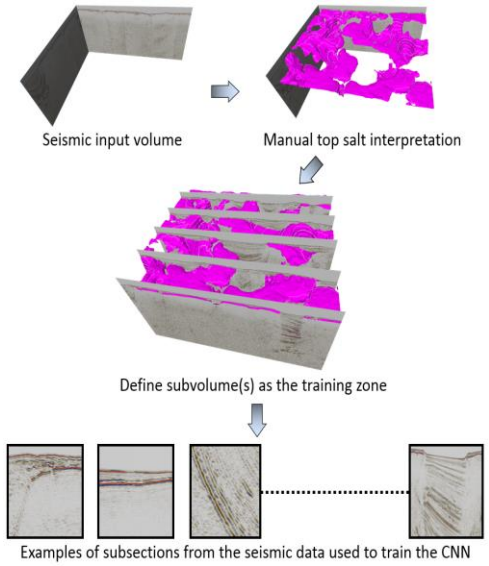

Figure 2: The training data are extracted as a subset from the seismic input volume and the corresponding manual interpretation of the top of salt.

The architecture of the convolutional neural network consists of 11 convolutional layers followed by ReLu nonlinearities and we use the common cross-entropy loss to evaluate the similarity between the network prediction and the ground truth. Training is performed for 30 epochs.

10.1190/segam2018-2996306.1

Automated interpretation of top and base salt

Evaluating the trained CNN for top salt interpretation

After the training has converged, the trained CNN is evaluated on the entire seismic survey including the 15% used for training. The top salt location is predicted by applying the trained CNN over the whole seismic survey and the result is then evaluated against the manual interpretation of top-of-salt. We obtain a coverage of approximately 92% where the two interpretations concur within a vertical distance of +/-2 samples corresponding to +/-64 ft. Figure 3 shows a comparison between the manually and the automatically extracted top salt interpretations.

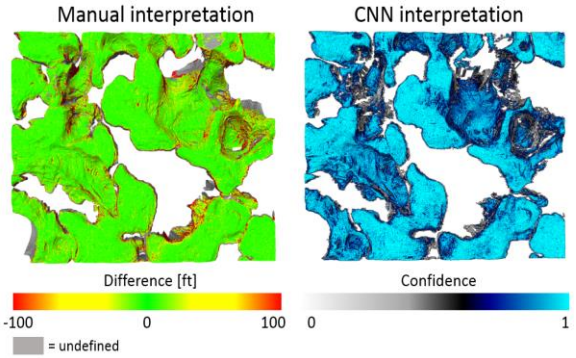

Figure 3: Comparison between the manual interpretation and the automated interpretation obtained from the trained CNN. The left figure shows the manual interpretation superimposed with a vertical difference map between the two interpretations in the range of +/- 100 ft, where the yellow and green colors represent a vertical difference within +/-2 samples. The right figure shows the top salt surface extracted by the CNN with a confidence map superimposed. These values are the output values from the CNN, where '0' is a highly uncertain/no match and '1' is a certain match.

In the second scenario, we apply the trained CNN on a seismic data volume from another survey, which is not included in the training data, to verify how well the network performs. We predict the top salt location, extract the corresponding top salt surface, and evaluate the result against the corresponding manual interpretation. We obtain a coverage of approximately 82%. This is a large survey covering an extent of approximately 26.000 km2. Figure 4 shows a comparison of the manual interpretation and the CNN-extracted top salt surface.

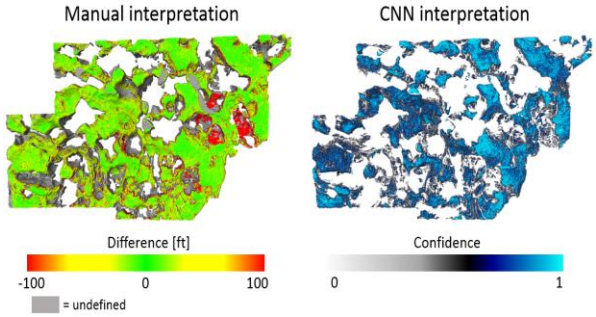

Figure 4: Comparison between the manual and automated interpretation of top of salt produced on a large seismic survey that was not included in training the CNN. The left figure shows the manual interpretation with a vertical difference map and the right figure shows the CNN extracted top salt surface with the confidence map superimposed. Both maps are scaled equally to the two attribute maps in Figure 3.

Training of a CNN for base salt interpretation

A convolutional network with the same architecture as for top of salt is trained for the base of salt. The training data are picked along a manual interpretation of the base in a salt flood volume within the same region that is used for the top of salt. In general, there are stronger lateral variations in the seismic signal along the base of salt compared to the top of salt. Some parts of the base have a strong seismic response with a certain lateral extent and connectivity. These zones might be tracked locally by an automated surface tracking tool based on a set of manual control points. Other parts of the base have often a more chaotic and weak seismic signal, making it difficult to define the interface between the salt zone and the sediments below. In these zones, a certain amount of manual interpretation, combined with interpolation, is required to build a complete base-of-salt surface. In this example, we remove all the interpolated parts of the manual interpretation and trained the convolutional network by picking training data along 15% of the non-interpolated zones. Figure 5 shows the manual interpretation after the interpolated zones were removed and how the training data are picked along the remaining strong-amplitude zones.

10.1190/segam2018-2996306.1

Automated interpretation of top and base salt

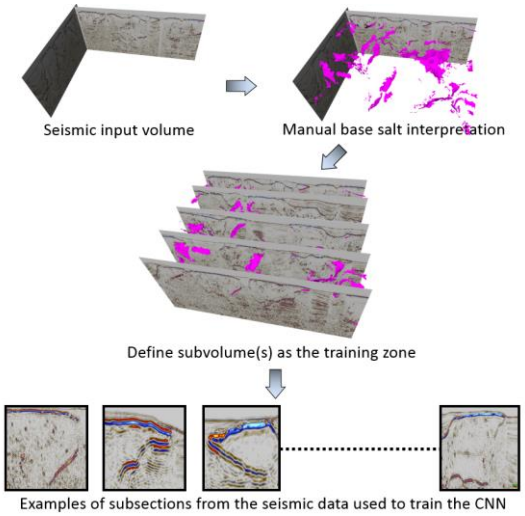

Figure 5: The training data are extracted as a subset from the seismic input volume and the corresponding manual interpretation of the base of salt. The interpolated parts of the manual interpretation of the base were removed and only zones with strong amplitude are considered in the training.

Evaluating the trained CNN for base salt interpretation

After the training has converged, the trained CNN for base of salt is used to automatically predict a base salt location for the entire seismic volume, including the 15% used for training, and the result is evaluated against the manual interpretation of base of salt. Figure 6 shows a comparison between the manually and the automatically extracted base salt interpretation.

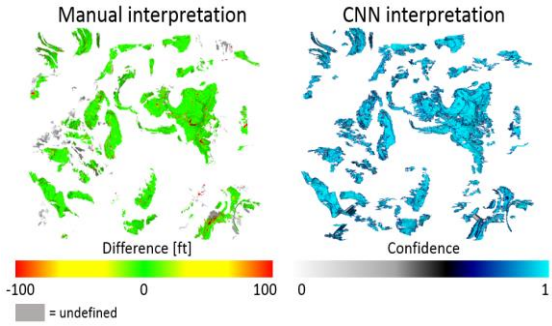

Figure 6: Comparison between the manual interpretation and the automated interpretation obtained from the trained CNN. The left panel shows the manual interpretation with a vertical difference map between the two interpretations in the range of +/- 100 ft, where the yellow and green colors represent a vertical difference within +/-2 samples. The right panel shows the base salt surface extracted by the CNN with a confidence map superimposed. These values are the output values from the CNN, where '0' is an uncertain match and '1' is a certain match.

We also apply the trained CNN for base of salt on a salt flood volume from another survey (the same survey used to evaluate the top of salt CNN). We predict the base salt surface and evaluated the result against the corresponding non-interpolated zones of the manual interpretation. Figure 7 shows a comparison of the manual interpretation and the CNN-extracted base salt surface.

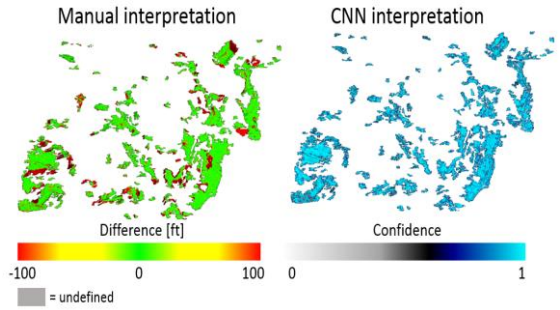

Figure 7: Comparison between the manual and automated interpretation of base of salt produced on a large seismic survey that was not included in training the CNN. The left panel shows the manual interpretation with a vertical difference map superimposed and the right panel shows the CNN extracted base salt surface with the confidence map superimposed.

Conclusions

We demonstrated that we can train two CNNs to successfully predict the location of the top salt surface for a given sediment flood volume and a base salt surface for a given salt flood volume. Currently, we achieve 92% coverage of the corresponding manual interpretation on the survey from which we picked training data. Furthermore, we showed that the trained CNN is general enough to also perform well on an input seismic data from a survey not included in training, obtaining 82% coverage. We also trained a CNN to predict the base-of-salt location for a given salt flood volume. We predicted the main parts of the base salt surface in the two salt flood volumes used in the evaluation. The main focus was to extract the regions with strong and distinct seismic amplitude signal along base salt. We are confident that we will improve the results both on top salt and base salt further by improving our CNN architecture and training procedures. The turnaround time to produce the results is reduced compared to manual interpretation and it can be reduced further using, e.g., virtual machines in a cloud solution.

Acknowledgements

The authors thank WesternGeco for permission to show real case data.

10.1190/segam2018-2996306.1

REFERENCES

Gramstad, O., and M. Nickel, 2018, Automated interpretation of top salt using deep convolutional nets: 80th Annual International Conference and Exhibition, EAGE, Extended Abstracts, https://doi.org/10.3997/2214-4609.201800731.

Gramstad, O., J. Haukaas, and J. O. H. Bakke, 2017, Automated salt interpretation: Part I—Extrema surface extraction guided by a DNA-inspired search method: 87th Annual International Meeting, SEG, Expanded Abstracts, 2071–2075, https://doi.org/10.1190/segam2017-17736226.1.

Haukaas, J., A. Bounaim, and O. Gramstad, 2017, Automated salt interpretation: Part 2—Smooth surface wrapping of volume attribute: 87th Annual International Meeting, SEG, Expanded Abstracts, 2076–2080, https://doi.org/10.1190/segam2017-17739151.1.

Waldeland, A. U., and A. H. S. S. Solberg, 2017, Salt classification using deep learning: 79th Annual International Conference and Exhibition, EAGE, Extended Abstracts, https://doi.org/10.3997/2214-4609.201700918.